

Short communication

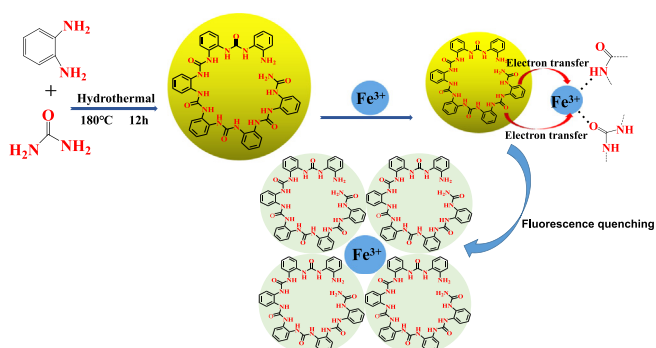
## Selective probes for ferric ion: A highly fluorescent nitrogen-doped carbon quantum dots

Liping Duan, Peng Wang, Miao Ren, Fang Liao\*

Chemical Synthesis and Pollution Control Key Laboratory of Sichuan Province, School of Chemistry and Chemical Industry, China West Normal University, Nanchong 637002, China



### GRAPHICAL ABSTRACT



### ARTICLE INFO

**Keywords:**  
N-CQDs  
Fluorescence probe  
Ferric ion detection  
One-step hydrothermal method

### ABSTRACT

Recently, carbon quantum dots (CQDs) is gaining more and more attention due to the possibility of its direct use in various fields of science and industry such as biomedical imaging, diagnostics and so on. In the paper, we successfully synthesized a nitrogen-doped carbon quantum dots (N-CQDs) with urea and *o*-phenylenediamine as raw materials by a facile and one-step hydrothermal method. The prepared N-CQDs was first used as fluorescent probe for the detection of iron(III) ion ( $\text{Fe}^{3+}$ ) and showed high selectivity and sensitivity. The detection mechanism of iron(III) ion ( $\text{Fe}^{3+}$ ) is further discussed. We assign the  $\text{Fe}^{3+}$  selectivity to the special coordinate interaction between  $\text{Fe}^{3+}$  and O,N of amide bond on the surface of N-CQDs. The detection limit was 39 nM. It showed excellent linear relationships in wide range from  $8 \times 10^{-7}$  to  $2.6 \times 10^{-6}$  M. The as-synthesized N-CQDs had been also successfully applied for cell imaging and detected  $\text{Fe}^{3+}$  in biosystem. It gave positive results when tested in both aqueous solution and living cells.

### 1. Introduction

The field of chemical sensing has always depended on novel materials, such as Polymers, nanomaterials and crystals [1]. As nanomaterials, organic dyes and semiconductor quantum dots are employed in biological application. However, semiconductor quantum dots may

lead to potential cytotoxicity because of heavy metal ions, and organic dyes have poor lightfastness [2]. Therefore fluorescent carbon-based nanomaterials include carbon quantum dots (CQDs) [4–7], carbon nanotubes [8], and fluorescent graphene [9], which have drawn increasing attention in recent years due to unique advantages such as biocompatibility, chemical stability, high optical absorptivity and low

\* Corresponding author.

E-mail address: [liaofang407@163.com](mailto:liaofang407@163.com) (F. Liao).

<https://doi.org/10.1016/j.inoche.2018.07.045>

Received 5 June 2018; Received in revised form 28 July 2018; Accepted 28 July 2018

Available online 15 August 2018

1387-7003/ © 2018 Elsevier B.V. All rights reserved.

toxicity [3]. The fluorescent carbon materials have superior properties than traditional fluorescent materials, and their applications have been broadened, such as medical diagnosis [10], photocatalysis [11], photovoltaic devices [12], bioimaging [2], and Biosensing [13]. So far, a number methods for preparing CQDs have been developed, such as arc discharge [14], hydrothermal method [15–19], laser irradiation [20], chemical oxidation [21], ultrasonic treatment [22], electrochemical synthesis [23], and microwave synthesis [24]. In recent years, hydrothermal method has been favored by researchers due to its simple operation, low cost and small environmental pollution [18].

Recently, due to its importance in the environmental and biological concern, metal ions have attracted the attention of researchers [25]. Such as Iron, it plays important roles in both biological and environmental media [26], as an important part of the heme group and the iron sulfur clusters, iron is an important element for various enzymatic reactions and for electron transfer in the respiratory chain [27]. Therefore, many methods have been proposed, such as spectrophotometry [28], cathodic stripping voltammetry [29], atomic absorption spectrometry [30], ion chromatography [31] and fluorescence spectrometry [27] used for the determination of iron in natural waters and biological systems [1,2,27,32]. Most of these methods are not only gruelling and time-consuming, but also require sample pretreatment procedures and intricate instrumentation [33]. Fluorescence analysis has distinct predominance, such as simplicity, nondestructive properties and high sensitivity. It has been widespread used in the detection of metal ions [4,6,34–36]. In addition, chemical sensors based on carbon quantum dots for detecting  $\text{Fe}^{3+}$  have also been reported. Qu and co-workers synthesized carbon quantum dots by hydrothermal treatment of dopamine. The surface of the prepared carbon quantum dots was rich in hydroquinone groups, it can be oxidized to the quinone species by iron and resulted in the fluorescence of carbon quantum dots quenching. Therefore, a sensitive trivalent iron chemical sensor was prepared with a detection limit of  $0.32 \mu\text{M}$  [37]. Liu and co-workers synthesized carbon quantum dots by hydrothermal treatment of alginate acid and ethanediamine. At the same time, the fabricated carbon quantum dots could be used to detect  $\text{Fe}^{3+}$  with the detect limitation of  $10.9 \mu\text{M}$  [38]. There were also several other carbon quantum dots chemical sensors used for  $\text{Fe}^{3+}$  detection reported. The carbon quantum dots prepared by using  $\beta$ -cyclodextrin, the mixture of isoleucine and citric acid, garlic as carbon precursors [39–41]. Thus, we proposed a fluorimetric method based on nitrogen doped carbon quantum dots to detect  $\text{Fe}^{3+}$ .

In this work, the nitrogen-doped carbon quantum dots (N-CQDs) was successfully synthesized by a facile and one-step hydrothermal method with urea and *o*-phenylenediamine. The prepared N-CQDs exhibited excitation wavelength-dependent photoluminescence, and the fluorescence of N-CQDs can be quenched by  $\text{Fe}^{3+}$ . In the range of 0 to  $50 \mu\text{M}$ , the PL intensity of the N-CQDs was decreased dramatically with the increase of concentrations of  $\text{Fe}^{3+}$ . The detection limit was  $39 \text{ nM}$  at room temperature. We also investigated the effects of  $\text{Fe}^{3+}$  on the PL of N-CQDs in cellular environment. The results demonstrate that N-CQDs can be applied for detecting  $\text{Fe}^{3+}$  in biosystem.

## 2. Synthesis of N-CQDs

*o*-Phenylenediamine aqueous solution was added into Urea aqueous solution, and next  $(\text{NH}_4)_2\text{S}_2\text{O}_8$  aqueous solution was added to the above mixed solution. Then transferred the mixed solution into a 50 mL Teflon-lined autoclave and maintained at  $180^\circ\text{C}$  for 12 h, and cooled naturally to room temperature. The products was separated and purified by centrifugation and dialysis. The detailed experimental section was mentioned in the supporting information.

## 3. Results and discussion

### 3.1. Characterization of the N-CQDs

Fig. 1a and c showed the magnification TEM image and particle size distribution histogram of N-CQDs, respectively. The HRTEM of Fig. 1b showed that the lattice spacing in the crystalline structure of N-CQD was  $0.205 \text{ nm}$ , it was close to the (103) diffraction plane of the diamond-like ( $\text{sp}^3$ ) carbon and matched the (102) diffraction plane of the  $\text{sp}^2$  graphitic carbon [48]. The result of Fig. 1b showed that the diameter of the N-CQDs is uniformly distributed from  $0.9$  to  $5.1 \text{ nm}$  and an average diameter is  $3.04 \text{ nm}$ .

Further inspection of the spectra was shown in Fig. S2 (a–e). It could be due to the  $\text{n}-\pi^*$  transition of N in the aromatic ring, resulting in the UV–vis absorption spectrum of N-CQD showed an absorption peak at  $413 \text{ nm}$  (Fig. S2e) [42]. The optimum excitation wavelength of the N-CQDs was approximately  $420 \text{ nm}$  and the optimum emission wavelength of the N-CQDs was  $566 \text{ nm}$  (Fig. S2a). As shown in Fig. S2b, the emission wavelength shifted  $1\text{--}3 \text{ nm}$  when the excitation wavelength increased from  $370$  to  $480 \text{ nm}$ . It showed that the prepared N-CQDs had good monodispersity in fluorescence intensity and size, and obviously different from other CQDs for analytical application [48]. Meanwhile, the emission intensity reached a maximum when excited at  $420 \text{ nm}$ . UV–vis and fluorescence spectra reflected the optical properties of N-CQDs. The fluorescence lifetime of N-CQDs was also measured. As shown in Fig. S2c, the fluorescence decay for N-CQDs was double-exponential with the weighted-average lifetime of  $2.75 \text{ ns}$ . The long decay component was  $4.59 \text{ ns}$  ( $42.03\%$ ), and the short decay component was  $1.41 \text{ ns}$  ( $57.97\%$ ). Moreover in Fig. S2d, the fluorescence decay for N-CQDs with  $\text{Fe}^{3+}$  was double-exponential with the weighted-average lifetime of  $2.82 \text{ ns}$ . The long decay component was  $5.06 \text{ ns}$  ( $37.64\%$ ), and the short decay component was  $1.47 \text{ ns}$  ( $62.36\%$ ). There is no energy and charge transfer between  $\text{Fe}^{3+}$  and N-CQDs due to the fluorescence lifetime without significant changes, the formation of a stable complex between ferric iron and N-CQDs may be the main cause of fluorescence quenching of N-CQDs.

In addition, the surface groups of the synthesized N-CQDs were also investigated using FT-IR (Fig. S3a) and XPS (Fig. S3c–f). As shown in Fig. S3a, the N-CQDs own characteristic absorption bands of N–H and O–H stretching vibrations at  $3440 \text{ cm}^{-1}$ , the C–H stretching vibrations at  $2930 \text{ cm}^{-1}$  and  $2850 \text{ cm}^{-1}$ . In the FT-IR spectrum, the peak at  $1630 \text{ cm}^{-1}$  demonstrated the presence of an amide bond [42], and C=N stretching vibrations at  $1380 \text{ cm}^{-1}$  in quinoid imine units [43], C–H out-of-plane bending vibration characteristic absorption peak at  $762 \text{ cm}^{-1}$  [44]. The Raman spectroscopy of the N-CQDs (Fig. S3b) showed two closely peaks at  $1356 \text{ cm}^{-1}$  (D band) and  $1531 \text{ cm}^{-1}$  (G band) of carbon respectively [45]. The XPS survey spectrum (Fig. S3f) of N-CQDs showed a C 1s peak at ca.  $284.54 \text{ eV}$ , an O 1s peak at ca.  $525.85 \text{ eV}$  and a N 1s peak at ca.  $398.59 \text{ eV}$ . The elemental composition of N-CQDs were C  $69.48\%$ , N  $27.08\%$  and O  $3.44\%$ , respectively. Fig. S3c showed the O 1s XPS spectrum of N-CQDs. It was mainly divided into two peaks, corresponding to signals of C=O ( $531.54 \text{ eV}$ ) and C–OH ( $534.2 \text{ eV}$ ). N 1s XPS spectrum (Fig. S3d) showed that there were also two peaks, which indicated the existence of C–N ( $398.57 \text{ eV}$ ) and N–H ( $400.3 \text{ eV}$ ) bonding models in N-CQDs. The C 1s XPS spectrum (Fig. S3e) demonstrated that the existence of C=O ( $288.2 \text{ eV}$ ), C–O ( $286.3 \text{ eV}$ ), C–N ( $285.03 \text{ eV}$ ), and C–C ( $284.01 \text{ eV}$ ) bonding models in N-CQDs [46–48]. Therefore, we could conclude that the as-prepared N-CQDs have abundant amide structure, slight hydroxyl on their surface.

### 3.2. Stability experiments of N-CQDs

As it is well known that the states of the particle surface affected the optical properties of N-CQDs. Different pH values may have different effects on the fluorescence intensity of N-CQDs. Therefore, the

Download English Version:

<https://daneshyari.com/en/article/7748283>

Download Persian Version:

<https://daneshyari.com/article/7748283>

[Daneshyari.com](https://daneshyari.com)